Degradation of 2-chlorophenol From Aqueous Solution by Soybean Residue Biochar Supported Sulfide-modified Nanoscale Zero-valent Iron Activated Persulfate

Ronghuan Xie
University of Science and Technology of China
Mu Wang
Hefei Engineering Research Center for Soil and Groundwater Remediation
Junjie Song
University of Science and Technology of China
Weiping Li (liweiping@mail.ustc.edu.cn)
Hefei Engineering Research Center for Soil and Groundwater Remediation https://orcid.org/0000-0002-4839-2854
Xiaodong Liu
University of Science and Technology of China

Research Article

Keywords: Biochar supported sulfide-modified nanoscale zero-valent iron, Persulfate, 2-chlorophenol, Degradation effect

Posted Date: March 22nd, 2022

DOI: https://doi.org/10.21203/rs.3.rs-1425514/v1

Abstract

In this work, soybean biochar supported sulfide-modified nanoscale zero-valent iron (BC@S-nZVI) was synthesized and used to activate persulfate (PS) for degrading 2-chlorophenol (2-CP) in aqueous solutions. Batch experiments were carried out to investigate the degradation effects under different conditions, including initial mass ratios among 2-CP, PS, and BC@S-nZVI, initial pH values, temperature, and anions. The results showed that the mass ratio of PS to 2-CP equaling 70 and the mass ratio of BC@S-nZVI to PS equaling 0.4 were the optimum mass ratios in the degradation system. The degradation efficiency of 2-CP was higher under acidic and alkaline conditions than the neutral condition, and the effect was best at the pH of 3, meanwhile, it increased with the increase of temperature. Moreover, the degradation rates were restrained with the addition of Cl^-, NO_3^- and CO_3^{2-}. The degradation process of 2-CP in BC@S-nZVI/PS system could be better described by a pseudo-second-order kinetic model than a pseudo-first-order kinetic model, and $SO_4\bullet^-$ was the predominant free radical under acidic conditions. The experimental results showed that it was promising to remove 2-CP from groundwater by PS activated with BC@S-nZVI.

Introduction

Chlorophenol compounds (CPCs) are frequently found in agricultural sites, water disinfected by chlorination, and pulp and paper mill effluents, which are carcinogens and widespread persistent organic pollutants in waters and soils (Vipul et al., 2021). As a priority pollutant, they are characterized as highly toxic, persistent, and easily mutagenic, and they can accumulate in organisms, such as algae, fishes, and mammals even humans (Nsh et al., 2021). 2-chlorophenol (2-CP), in particular, is one of the most representative chlorophenol compounds, which are highly stable and carcinogens because of their phenyl structure and the presence of chlorine and are listed as priority pollutants by China and the US Environmental Protection Agency (Li et al., 2020; Majumder and Gupta, 2007). The pollution of 2-CP in groundwater and wastewater should be concerned because of its toxicity and almost non-biodegradability. Removal of 2-CP from wastewater has been treated by biological and physicochemical methods (Loh and Wu, 2006; Miguel et al., 2018); these methods can effectively degrade 2-CP under certain conditions. However, the conventional methods are still problematic, such as when the content of 2-CP is relatively low, it cannot be completely degraded, or biodegradation requires strict environmental conditions. Therefore, it is urgently necessary to develop more widely applicable methods for 2-CP degradation.

In recent years, advanced oxidation processes (AOPs), including ozone (O_3), persulfate (PS) activation, and hydrogen peroxide (H_2O_2) activation, have been developed as highly promising methods for degrading toxic and recalcitrant organic compounds (Liu et al., 2017; Xl et al., 2021; Zhou et al., 2020). Among them, persulfate-based (peroxodisulfate, PDS, and peroxymonosulfate, PMS) advanced oxidation processes have been widely applied to remove organic contaminants in wastewater and groundwater (Chen et al., 2021; Liu et al., 2020). Persulfate is found more stable in the subsurface as compared to

H_2O_2 and O_3, for it persisted in the subsurface and can be injected at high concentrations, transported in porous media, and would undergo density-driven and diffusive transport into low-permeability materials (Huang et al., 2002). Under mild conditions, PS can be activated via photolysis (UV and visible), alkali, heat, electron beam, and transition metals, forming the hydroxyl radical (•OH) and sulfate radical anion ($SO_4•^-$)(Matzek and Carter, 2016; Muhammad et al., 2019; Peng et al., 2015; Wang and Wang, 2018). $SO_4•^-$ has a high reduction potential (E_0 = 2.5–3.1 V), and is nonselective compared with ·OH, and it can quickly mineralize most of the organic pollutants into inorganic compounds (Devi et al., 2016; Gao et al., 2012).

Transition metals have been widely applied to activate PS because of their effectiveness and cost-effectiveness(Wang et al., 2021). Among various transition metals, nanoscale zero-valent iron (nZVI) is considered a simple, economical, and environmentally friendly material, which can slow-release Fe^{2+} to activate PS (Kim et al., 2018). The removal efficiency of 2,4-dichlorophenol using the nZVI/PS system was better than those of the Fe^{2+}/PS and nFe_3O_4/PS; the maximum degradation rate reached around 92.5% within 150 min (Li et al., 2015). However, nZVI catalysis has low PDS activation efficiency because of its aggregation, passivation, and poor electron transfer(Zhao et al., 2019b).

To improve stability, various porous media (e.g., coal fly ash (Chen et al., 2018), clay minerals (Li et al., 2016), carbon-based materials (Pirsaheb et al., 2018)) have been applied as supports of nZVI to boost their reactivity. Biochar (BC) is considered one of the best carriers for nZVI due to its low cost, porous structure, and high surface area (Hao et al., 2021; Kumar et al., 2021). However, this method is characterized by low degradation efficiency due to slow electron transfer rate and passivation induced by biochar (Dong et al., 2018; Vogel et al., 2019). Recently, some studies have reported a sulfide-modified method to improve the removal efficiency, which ascribes to the enhancements of hydrophobicity of nZVI, production of •OH, and salt resistance (Cai and Zhang, 2021; Wu et al., 2021; Xu et al., 2019). The presence of sulfur could regulate the morphology of S-mZVI with a dispersed and spherical shape, and it could improve the activation performance of PS (Zhang et al., 2021). The feasibility and mechanism of sulfide-modified nanoscale zero-valent iron supported on biochar for the removal of TCE in groundwater remediation is investigated; the results showed that the BC@S-nZVI, combining the high adsorption capacity of BC and the high reductive capacity of S-nZVI, had a much better performance than the single S-nZVI or BC (Chen et al., 2020). Therefore, sulfide-modified nZVI (S-nZVI) catalysts have been paid more and more attention, and it is of great significance to explore the new S-nZVI composite using BC and improve its efficiency in practical application.

In this study, soybean residue biochar supported S-nZVI (BC@S-nZVI) synthesized in a one-step method has been developed to activate PS for the degradation of 2-CP in an aqueous solution. The effects of initial concentration values of 2-CP and PS, BC@S-nZVI doses, pH values, reaction temperature, and some anion concentration values on degradation efficiency were also investigated. Furthermore, the degradation mechanism and the contribution of each chemical factor in the reaction system have also been explored using scavengers of radicals under optimum mass ratios of PS and BC@S-nZVI.

Materials And Methods

Chemicals and reagents

2-chlorophenol (2-CP, $C_6H_5OCl \geq 98.5\%$), iron nitrate nonahydrate ($Fe(NO_3)_3–9H_2O \geq 98.5\%$), sodium sulfide ($Na_2S–9H_2O \geq 98.5\%$), and tert-butyl alcohol (TBA, $C_4H_{10}O \geq 98.0\%$) were chemically pure reagents, purchased from Sinopharm Chemical Reagent Co., Ltd., China. Sodium persulfate (PS, $Na_2S_2O_8 \geq 99.0\%$) and potassium borohydride (PBH, $KBH_4 \geq 99.0\%$) were analytical reagents, bought from Shanghai Macklin Biochemical Co., Ltd. Hydrochloric acid (HCl, 36.0%~38.0%), sodium hydroxide (NaOH ≥ 99.0%), sodium chloride (NaCl ≥ 99.5%), sodium carbonate ($Na_2CO_3 \geq 99.5\%$) and sodium nitrate ($NaNO_3 \geq 99.5\%$) were analytical reagents, obtained from Tianjin Kermel Chemical Reagent Co., Ltd.. Methanol (MeOH, $CH_4O \geq 99.9\%$), and methylene chloride (DCM, $CH_2Cl_2 \geq 99.9\%$) were guarantee reagents, purchased from Shanghai Weston Trading Co., Ltd. The ultra-pure water for the preparation of aqueous solutions in all experiments of this study was produced by Merck Millipore Synergy UV.

Synthesis of BC@S-nZVI

Soybean residue was collected in the soybean processing factory from Hefei. It was dried for 24 hours before being used. The dried soybean residue was then placed in a tube heating furnace with the model OTF-1200X. The temperature was raised from 0 to 800 ℃ in one hour at a heating rate of 14 ℃/min, kept for half an hour, and dropped to room temperature in four hours with nitrogen flushing in the whole process. After cooling down, the obtained BC was ground and passed a 50-mesh sieve.

BC@S-nZVI was synthesized in a one-step method. 3.472g BC were added to 0.31 M $Fe(NO_3)_3$ solution of 200 mL, stirring constantly for 30 minutes, and nitrogen was pumped into the solution. Then, 3.1 M PBH solution of 200 mL was added into the suspension liquid dropwise. After stirring for 10 minutes, 0.14 M Na_2S solution of 110 mL was added into the mixed solution and treated by ultrasound for 30 minutes. The solution was pumped through a Bouchard funnel, and the filter residue was cleaned with ultra-pure water until the conductivity dropped below 50 μS/cm. Lastly, the material was dried in a freeze dryer in which the mass ratio of nZVI-to-C was 1:1, and S-to-Fe was 1:7.

Experimental process

2-CP and PS solutions were prepared using ultra-pure water. All reaction systems were carried out in 40 mL vials with Teflon covers and initiated with 20 mL 2-CP solution. Then, BC@S-nZVI and PS solutions were added to the solution. The vials were shaken at 180 rpm in a thermostatic reciprocating shaker (model of SHA-B) at various reaction temperatures. The samples were collected at different reaction time (10 min, 30 min, 1 h, 2 h, 4 h, 8 h, 16 h, 24 h, 48 h, and 72 h) and filtered through 0.22 mm membranes to determine 2-CP concentration which was extracted into DCM. The extraction process was as follow: The reaction solution of 5 mL was taken in the sample bottle in which MeOH reagent of 0.2 mL was added. Then 2 drops of concentrated HCl was added in the bottle to make the solution pH value less than 2. After that, NaCl reagent of 0.5 g and DCM reagent of 5 mL were added successively. The bottle was shaken at

180 rpm for 20 minutes, then stood for 10 min. Finally, the solution of 1mL from the lower layer was injected into a sample vial with a syringe and capped it for determining.

This study set the mass ratio of PS to 2-CP to 0, 50, 60, 70, and 80, the mass ratio of BC@S-nZVI to PS to 0, 0.4, 0.8, 1.0, and 1.5 with 2-CP concentration values of 20, 50, and 100 ppm in the experiments. PH values were designed as 3.0, 5.0, 7.0, 9.0 and 11.0, temperature values were designed as 10 ℃, 30 ℃, and 50 ℃, anions including chloride ions, nitrate ions, and carbonate ions were designed as a concentration of 0, 30, 50, 100, 300 and 500 ppm. All experiments were conducted with duplicate samples.

Analytical methods

The surface features of the BC@S-nZVI before and after reactions were observed using a scanning electron microscope (SEM) (TESCAN MIRA 3 LMH FE-SEM, Czech Republic) in the CAS Key Laboratory of Crust-Mantle Materials and Environments, University of Science and Technology of China. The cathode luminescence was launched using a CL probe (Gatan Chromal CL2, England), and the surface composition of BC@S-nZVI was characterized using X-ray photoelectron spectroscopy (XPS, EDAX GENESIS APEX Apollo System, America). The scanning sizes included 1 mm, 2 mm, 5 mm, 10 mm, and 20 mm.

The concentration of 2-CP was determined by a gas chromatography (Shimadzu Nexis GC-2030, Japan) in the Hefei Engineering Research Center for Soil and Groundwater Remediation. Chromatographic conditions were as follows. Column: SH-RTX-5 (30 m×0.32mm×0.25 mm), FID detector, detector temperature: 300°C, injection volume: 1 μL, inlet temperature: 250°C, splitter ratio: 2:1, column flow rate: 1.5 mL /min, heating procedure: keeping 50℃ for 5min, then increased to 140°C by a heating rate of 10°C/min, the detection limit of 2-CP was 5 μg/L.

The pH of the aqueous solution was measured by PHBJ-260 pH composite electrode, which was purchased from Shanghai INESA Scientific Instrument Co., Ltd. Cleaning the probe of pH-meter with ultra-pure water firstly, then the aqueous solution was shaken to be even. After that, the cap was opened, and the probe was inserted to one-third of the distance from the bottom of the vial and started to measure the pH. After the instrument indicated that the measurement was completed with the pH value recorded, the probe was taken out. The probe was cleaned with ultra-pure water again to end the measurement.

The conductivity of the aqueous solution for cleaning the filter residue was measured by the DDS-307 conductivity meter, which was purchased from Shanghai INESA Scientific Instrument Co., Ltd. Cleaning the probe of conductivity meter with ultra-pure water firstly, then the aqueous solution was shaken to be even, the probe was inserted to one-third of the distance from the bottom of the beaker and pressed the measurement button to measure the conductivity. The probe was taken out after the measured value displayed by the instrument did not change, the conductivity value was recorded, and the probe was cleaned with ultra-pure water.

Results And Discussion

Characteristic of BC@S-nZVI composite

SEM images of BC@S-nZVI before and after the reaction are shown in Fig. 1. It was evident that BC@S-nZVI had a honeycomb-like and porous structure from different grades before reaction (Fig. 1(a) and (c)). After the reaction, there were many smooth images on the surface of the material, which was the result of S-nZVI shedding or degradation products filling in the sites during the reaction process (Fig. 1(b) and (d)). This illustrated that BC provided vast binding sites and effectively prevented the agglomeration of S-nZVI; it was conducive to activating PS to generate free radical degradation of 2-CP.

Effects of PS and BC@S-nZVI doses

The masses of PS and BC@S-nZVI were the most critical parameters in the degradation system of 2-CP. To investigate the relationship among the three parameters reasonably, the mass concentration was adjusted by setting the mass ratio of PS to 2-CP and BC@S-nZVI to PS to obtain the optimum mass ratios suitable for different initial concentrations of 2-CP. The mass ratio of PS to 2-CP included 0, 50, 60, 70, and 80; the mass ratio of BC@S-nZVI to PS included 0, 0.4, 0.8, 1.0, and 1.5. The relationship between $\ln(C/C_0)$ of 2-CP with the mass concentration of PS and BC@S-nZVI are shown in Fig. 2.

The influences of mass ratio of PS to 2-CP on the degradation of 2-CP are shown in Fig. 2 (a), when the PS dosage increased from 0 to 1400 ppm with the mass ratio of PS to 2-CP changed from 0 to 70 and the mass concentration of BC@S-nZVI equalled to 560 ppm, the removal rate of 2-CP increased from 9.2–100.0% in 72 h, indicating that higher PS dosage was beneficial to the degradation of 2-CP. The radical was generated due to the activation of PS by BC@S-nZVI, which means that increasing the dosage of PS would promote the production of oxidative species, leading to higher 2-CP removal rates. However, the degradation efficiency of 2-CP decreased when the PS dosage was increased to 1600 ppm, with the mass ratio of PS to 2-CP increased to 80. It can be attributed to the consumption of $SO4^{\bullet-}$ by the reaction with each other or PS (Yousefi et al., 2019; Zhu et al., 2020). Therefore, the mass ratio of PS to 2-CP equaling 70 was selected as the optimum dosage of PS for further experimentation.

The influences of the mass ratio of BC@S-nZVI to PS on the degradation of 2-CP were shown in Fig. 2 (b). When the mass concentration of BC@S-nZVI increased from 0 to 560 ppm with the mass ratio of BC@S-nZVI to PS changed from 0 to 0.4, the removal rate of 2-CP increased from 22.3–100.0% in 72 h, continuously increased the mass ratio of BC@S-nZVI to PS to 1.5, the degradation efficiency of 2-CP was improved and the complete removal time reduced to 24 h. However, BC@S-nZVI was considered a catalyst, and the mass concentration should not be too high in this study. Therefore, the mass ratio of BC@S-nZVI to PS was set to 0.4 while the mass ratio of PS to 2-CP equaling to 70 was selected as the optimum mass ratio in the degradation system of 2-CP.

Effects of initial concentration values of 2-CP and different reaction systems

Different 2-CP concentration values of 20, 50, and 100 ppm were set, contrast experiments were carried out to investigate the effects of various reaction systems. The results are shown in Fig. 3.

The degradation effects of different initial concentration values of 2-CP are shown in Fig. 3 (a). When concentration values of 2-CP increased from 20 ppm to 100 ppm, PS dosage and mass concentration of BC@S-nZVI increased with it. With the optimum mass ratios being constant, the removal efficiency was improved, but the total removal time remained 48 h. Therefore, it was evident that the optimum mass ratios were applicable with the change of initial concentration value of 2-CP.

The degradation effects of eight various reaction systems are contrasted in Fig. 3 (b); they were BC@S-nZVI/PS, BC@S-nZVI, BC@nZVI/PS, BC@nZVI, S-nZVI/PS, S-nZVI, nZVI/PS, and nZVI in 2-CP aqueous solution with 20 ppm of 20 mL, respectively. The removal efficiencies of reaction systems in the presence of PS were higher than those without PS, and BC@S-nZVI/PS showed the best efficiency among them, then was S-nZVI/PS, 2-CP were completely removed in 48 h of them otherwise many residues in other systems. This indicated that the introducing of S and BC on nZVI considerably activated PS and produced more free radicals for degradation of 2-CP while they don't have much degradability of their own.

Therefore, BC@S-nZVI/PS system showed a higher degradation rate of 2-CP than other reaction systems, and the optimum mass ratios were applicable of different initial concentration values of 2-CP.

Effects of initial solution pH and temperature values

The values of pH and temperature were essential factors that affected 2-CP degradation. Batch experiments of variational pH and temperature were carried out at the optimum mass ratios, and the results are shown in Fig. 4.

Different pH values influenced the degradation of 2-CP in BC@S-nZVI/PS system are shown in Fig. 4 (a), the degradation rate of 2-CP decreased from acidic and alkaline conditions to the neutral condition. The removal rate of 2-CP reached 100.0% for the pH value of 3, 5, and 11 after a reaction time of 16 h, 48 h, and 72 h, respectively. The degradation rate of 2-CP was only 64.5% for the pH value of 7. The results indicated that the acidic condition had a more positive effect on removing 2-CP than the neutral and alkaline conditions. Furthermore, BC@S-nZVI was corroded to form Fe^{2+} as the activator of PS to generate $SO4•^{-}$ under acidic conditions. Some researchers have found that the activation energy required to activate PS can be reduced under acidic conditions; this resulted in the activation process being accelerated, and the 2-CP degradation being enhanced (Manz and Carter, 2017).

The values of temperature that influenced the degradation of 2-CP in BC@S-nZVI/PS system are shown in Fig. 4 (b), the degradation rate of 2-CP decreased with the decrease of temperature from 50 ℃ to 10 ℃. When the temperature was 50 ℃, 100.0% of 2-CP was removed within 16 h, whereas the removal rate was only 23.7% at 10 ℃ within 72 h, this was consistent with some reports that higher temperature had a positive effect on the activation of PS and the degradation of contaminants (Zhao et al., 2019a).

Effects of inorganic anions of chloride, carbonate, and nitrate

The composition of actual wastewater was quite complex, and inorganic anions may coexist, affecting pollutants' degradation (Wang et al., 2019). Batch experiments were carried out to clarify the effect of inorganic anions Cl^-, NO_3^- and CO_3^{2-} on the degradation of 2-CP in the BC@S-nZVI/PS system. The results are shown in Fig. 5. It was observed in Fig. 5(a) that the degradation of 2-CP was slightly restrained with the addition of Cl^-. The degradation of 2-CP was 100.0% without Cl^- in the aqueous solution within 48 h. It had the minimal impact on the degradation rate of 2-CP when the concentration of Cl^- was 100 ppm which 94.4% of 2-CP was removed within 72 h, whereas the removal rate was only 71.0% at 30 ppm within 72 h. Chlorine radicals could be generated due to the chain reaction of Cl^- and $SO_4•^-$ and it had a weaker activity than that of SO4•⁻. Consequently, the presence of Cl^- showed a slightly negative effect on the degradation of 2-CP.

It was observed in Fig. 5(b) that the degradation of 2-CP was restrained with the addition of NO_3^-. The degradation of 2-CP was 100.0% without NO_3^- in the aqueous solution within 48 h. It had the minimal impact on the degradation rate of 2-CP when the concentration of NO_3^- was 50 ppm which 90.4% of 2-CP was removed within 72 h, whereas the removal rate was only 59.8% at 500 ppm within 72 h. Some previous research showed NO_3^- had a low reactivity with SO4•⁻ to generate a less reactive radical, leading to the formation of a passive layer on the surface of nZVI (Gao et al., 2018; Huang et al., 2019). As a result, the presence of NO_3^- showed a negative effect on the degradation of 2-CP.

It was observed in Fig. 5(c) that the degradation of 2-CP was restrained with the addition of CO_3^{2-}. The degradation of 2-CP was 100.0% without CO_3^{2-} in the aqueous solution within 48 h. It had the minimal impact on the degradation rate of 2-CP when the concentration of CO_3^{2-} was 300 ppm which 97.2% of 2-CP was removed within 72 h, whereas the removal rate was only 68.7% at 30 ppm within 72 h. Some reports showed carbonate radical could be generated due to the reaction of CO_3^{2-} and SO4•⁻, it reacted rapidly with phenol substance at high concentration and showed a negative effect with constant consumption (Wang and Lin, 2012).

2-CP degradation mechanism in the BC@S-nZVI/PS system

The experimental data of the optimum mass ratios were fitted with a pseudo-first-order model and a pseudo-second-order model to explore the degradation mechanism of 2-CP by BC@S-nZVI/PS, and the result is shown in Fig. 6.

It was observed in Fig. 6 that there were two stages of the degradation of 2-CP with reaction time in the BC@S-nZVI/PS system. The first stage was the rapidly reacting stage, and the degradation amount reached 16.1 ppm after 24 h, mainly because the active sites were sufficient of BC@S-nZVI, and 2-CP could fully contact them; on the other side, PS was activated to produce a lot of active free radicals,

degradation reaction was rapidly conducted. In the second stage, a large amount of PS was consumed, and the active surface sites of S-nZVI were gradually saturated. As a result, the degradation of 2-CP by BC@S-nZVI/PS reached a balance in 72 h.

Experimental data of the optimum mass ratios fit well with the pseudo first-order kinetic model and the pseudo-second-order kinetic model. However, the correlation coefficient R^2 and equilibrium absorption mass Q_e of the pseudo-second-order kinetic model were larger than a pseudo-first-order kinetic model, the theoretical degradation mass 19.90751 ppm of the pseudo-second-order kinetic model was closer to the experimental equilibrium absorption mass 20 ppm, this meant that pseudo-second-order kinetic model could better describe the degradation process of 2-CP in BC@S-nZVI/PS system than a pseudo-first-order kinetic model. The pseudo-second-order kinetic model was mainly related to chemical adsorption, and the main influencing factor was the formation of chemical bonds between 2-CP and BC@S-nZVI/PS. Therefore, the adsorption process of 2-CP was a joint action of many mechanisms, mainly was chemical action.

The experiments of the optimum mass ratios of PS and BC@S-nZVI, added 0.8 mL TBA in the optimum mass ratios to quench •OH, added 0.8 mL MeOH in the optimum mass ratios to quench •OH and $SO4•^-$, added optimum PS ratios alone, and added optimum BC@S-nZVI ratios alone were carried on for analyzing the contribution rates of the chemical factors during the 2-CP degradation process. The results are shown in Fig. 7.

It was observed in Fig. 7(a) that the experiment of highest degradation rate was optimum mass ratios of PS and BC@S-nZVI, which had 100.0% degradation rate in 48 h, then the degradation rate from high to low was added TBA, added MeOH, added PS alone, and added BC@S-nZVI alone, respectively. The analysis revealed •OH was quenched after TBA was added in the optimum mass ratios, •OH and $SO4•^-$ were quenched after MeOH was added in the optimum mass ratios; it could be concluded that the effect of $SO4•^-$ was stronger than that of other chemical factors, and the effect of oxidation of activated PS was stronger than that of adsorption of BC@S-nZVI and reductive dichlorination of nZVI in degrading 2-CP.

The degradation rate of 2-CP in each group while the reaction reached equilibrium (72 h) was quantified analysis to explore the contribution rate of each chemical factor in the process of 2-CP degradation, and the result is shown in Fig. 7(b), they were 100.0%, 79.8%, 40.1%, 22.2% and 9.2% under the condition of optimum mass ratios of PS and BC@S-nZVI, with TBA, MeOH, PS, and BC@S-nZVI added respectively. The contribution rate of each chemical factor was calculated; $SO4•^-$ had the most significant contribution rate with 39.7% of each chemical factor, the contribution rates were 20.1%, 22.3%, 9.2%, and 8.7% of •OH, oxidation of activated PS, adsorption of BC@S-nZVI and reductive dichlorination of nZVI, respectively. This indicated that $SO4•^-$ was the predominant free radical in the BC@S-nZVI/PS system under acidic conditions in the degradation of 2-CP.

Conclusions

In this study, soybean residue biochar supported S-nZVI (BC@S-nZVI) was synthesized in a one-step method and has been used as an activator of persulfate (PS) to remove 2-chlorophenol (2-CP) in the aqueous solution. Batch experiments were carried on to investigate the degradation effects under different conditions, including reaction system and background in the aqueous solution, the degradation mechanism of 2-CP was discussed and the conclusions are as follows.

Activation of persulfate through the method of supporting sulfide-modified nanoscale zero-valent iron by soybean residue biochar could improve the degradation effect of 2-CP in the aqueous solution. The mass ratio of PS to 2-CP equaling to 70, the mass ratio of BC@S-nZVI to PS equaling to 0.4 were the optimum mass ratios in the degradation system, and the degradation rate of 2-CP could reach 100.0% in 72 h.

The BC could provide massive binding sites and effectively prevent the agglomeration of S-nZVI. The degradation efficiency of 2-CP decreased gradually from acidic and alkaline conditions to the neutral condition, and the effect was best when the pH was 3 and increased with the increase of temperature. The degradation of 2-CP was restrained with the addition of Cl^-, NO_3^-, and CO_3^{2-}, the concentration of least effect was 100 ppm, 50 ppm, and 300 ppm, respectively. This was mainly due to the consumption of SO4•⁻ by inorganic anions to generate less reactive radicals in the degradation process. Simulation of adsorption kinetics indicated that the degradation process of 2-CP in BC@S-nZVI/PS system could be better described by a pseudo-second-order kinetic model than a pseudo-first-order kinetic model, and SO4•⁻ was the predominant free radical under acidic conditions.

This study could provide helpful guidance about the degradation of chlorophenol pollutants by the BC@S-nZVI/PS system, and this system could be used for groundwater remediation of in-situ chemical oxidation (ISCO).

Declarations

The authors declare that they have no known competing financial interests or personal relationships that could have appeared to influence the work reported in this paper.

Funding

This study is thankful for the support of the Major Science and Technology Project of Anhui Province (202003a06020024) and Hefei Key Technology Major Research and Development Projects (2021GJ063).

Author Contributions

Ronghuan Xie: Pot experiment setup, Sampling, Investigation, Writing and editing. **Mu Wang:** Methodology, Amendment material preparation, Pot experiment setup, Sampling, Investigation, Formal analysis, Writing - original draft. **Junjie Song:** Methodology, Software. **Weiping Li**: Conceptualization, Methodology, Writing- review and editing, Funding acquisition. **Xiaodong Liu**: Conceptualization, Writing - review and editing. All authors read and approved the final manuscript.

Ethical approval

Not applicable.

Consent to participate

Not applicable.

Consent to publish

Not applicable.

Competing Interests

The authors have no relevant financial or non-financial interests to disclose.

Availability of data and materials

The datasets generated during and/or analyzed during the current study are available from the corresponding author on reasonable request.

References

1. Cai J, Zhang Y (2022) Enhanced degradation of bisphenol S by persulfate activated with sulfide-modified nanoscale zero-valent iron. Environ Sci Pollution Res 29(6):8281–8293. https://doi.org/10.1007/s11356-021-16156-8
2. Chen CY, Cho YC, Lin YP (2021) Activation of peroxydisulfate by carbon nanotube for the degradation of 2,4-dichlorophenol: Contributions of surface-bound radicals and direct electron transfer. Chemosphere 283:131282. https://doi.org/10.1016/j.chemosphere.2021.131282
3. Chen J, Dong HR, Tian R, Li R, Xie QQ (2020) Remediation of Trichloroethylene-Contaminated Groundwater by Sulfide-Modified Nanoscale Zero-Valent Iron Supported on Biochar: Investigation of Critical Factors. Water Air and Soil Pollution 231(8):432. https://doi.org/10.1007/s11270-020-04797-3
4. Chen Z, Xing J, Pu Z, Wang X, Yang S, Wei B, Ai Y, Xiang L, Chen D, Wang X (2018) Preparation of nano-Fe^0 modified coal fly-ash composite and its application for U(VI) sequestration. J Mol Liq 266:824–833. https://doi.org/10.1016/j.molliq.2018.05.118
5. Devi P, Das U, Dalai AK (2016) In-situ chemical oxidation: Principle and applications of peroxide and persulfate treatments in wastewater systems. Sci Total Environ 571:643–657. https://doi.org/10.1016/j.scitotenv.2016.07.032
6. Dong HR, Zhang C, Deng JM, Jiang Z, Zhang LH, Cheng YJ, Hou KJ, Tang L, Zeng GM (2018) Factors influencing degradation of trichloroethylene by sulfide-modified nanoscale zero-valent iron in aqueous solution. Water Res 135:1–10. https://doi.org/10.1016/j.watres.2018.02.017

7. Gao YQ, Gao NY, Deng Y, Yang YQ, Ma Y (2012) Ultraviolet (UV) light-activated persulfate oxidation of sulfamethazine in water - ScienceDirect. Chem Eng J 195–196:248–253. https://doi.org/10.1016/j.cej.2012.04.084
8. Gao YQ, Gao NY, Wei W, Kang SF, Xu JH, Xiang HM, Yin DQ (2018) Ultrasound-assisted heterogeneous activation of persulfate by nano zero-valent iron (nZVI) for the propranolol degradation in water. Ultrason Sonochem 49:33–40. https://doi.org/10.1016/j.ultsonch.2018.07.001
9. Hao X, Mengxi G, Xi H, Yonghua C, Yan L, Xinyu X, Riqing Z, Xiong Y, Chunfang T, Xinjiang H (2021) A novel preparation of S-nZVI and its high efficient removal of Cr(VI) in aqueous solution. J Hazard Mater 416:125924. https://doi.org/10.1016/j.jhazmat.2021.125924
10. Huang J, Yi S, Zheng C, Lo I (2019) Persulfate activation by natural zeolite supported nanoscale zero-valent iron for trichloroethylene degradation in groundwater. Sci Total Environ 684:351–359. https://doi.org/10.1016/j.scitotenv.2019.05.331
11. Huang KC, Couttenye RA, Hoag GE (2002) Kinetics of heat-assisted persulfate oxidation of methyl tert-butyl ether (MTBE). J Soil Contam 11:447–448. https://doi.org/10.1016/S0045-6535(02)00330-2
12. Kim CL, Ahn JY, Kim TY, Shin WS, Hwang I (2018) Activation of Persulfate by Nanosized Zero-Valent Iron (NZVI): Mechanisms and Transformation Products of NZVI. Environ Sci Technol 52:3625–3633. https://doi.org/10.1021/acs.est.7b05847
13. Kumar NS, Shaikh HM, Asif M, Al-Ghurabi EH (2021) Engineered biochar from wood apple shell waste for high-efficient removal of toxic phenolic compounds in wastewater. Sci Rep 11:2586. https://doi.org/10.1038/s41598-021-82277-2
14. Li N, Chen HD, Lu YZ, Zhu MC, Zeng RJ (2020) Nanoscale zero-valent iron-modified PVDF membrane prepared by a simple filter-press coating method can robustly remove 2-chlorophenol from wastewater. Chem Eng J 416:127701. https://doi.org/10.1016/j.cej.2020.127701
15. Li RC, Jin XY, Megharaj M, Naidu R, Chen ZL (2015) Heterogeneous Fenton oxidation of 2,4-dichlorophenol using iron-based nanoparticles and persulfate system - ScienceDirect. Chem Eng J 264:587–594. https://doi.org/10.1016/j.cej.2014.11.128
16. Li X, Zhao Y, Xi B, Mao X, Gong B, Li R, Peng X, Liu H (2016) Removal of nitrobenzene by immobilized nanoscale zero-valent iron: Effect of clay support and efficiency optimization. Appl Surf Sci 370:260–269. https://doi.org/10.1016/j.apsusc.2016.01.141
17. Liu P, Guo ZP, Wang YD, Zhang L, Xue G (2017) Enhanced decolorization of methyl orange in aqueous solution using iron-carbon micro-electrolysis activation of sodium persulfate. Chemosphere: Environ Toxicol risk Assess 180:100–107. https://doi.org/10.1016/j.chemosphere. 2017.04.019
18. Liu Y, Zhao Y, Wang J (2020) Activation of peroxydisulfate by a novel Cu0-Cu2O@CNTs composite for 2, 4-dichlorophenol degradation. Sci Total Environment:141883 https://doi.org/10.1016/j.scitotenv.2020.141883
19. Loh KC, Wu TT (2006) Cometabolic Transformation of 2-Chlorophenol and 4-Chlorophenol in the Presence of Phenol by Pseudomonas putida. Can J Chem Eng 84:356–367.

https://doi.org/10.1002/cjce.5450840312

20. Majumder PS, Gupta SK (2007) Removal of chlorophenols in sequential anaerobic–aerobic reactors. Bioresour Technol 98:118–129. https://doi.org/10.1016/j.biortech.2005.11.009
21. Manz KE, Carter KE (2017) Investigating the effects of heat activated persulfate on the degradation of furfural, a component of hydraulic fracturing fluid chemical additives. Chem Eng J 327:1021–1032. https://doi.org/10.1016/j.cej.2017.06.168
22. Matzek LW, Carter KE (2016) Activated persulfate for organic chemical degradation: A review. Chemosphere 151:178–188. https://doi.org/10.1016/j.chemosphere.2016.02.055
23. Miguel MJ, Sergio MH, Anne-Claire T, Flor CL (2018) 2-Chlorophenol consumption by cometabolism in nitrifying SBR reactors. Chemosphere 212:41–49. https://doi.org/10.1016/j.chemosphere.2018.08.064
24. Muhammad A, Klu PK, Wang C, Zhang W, Luo R, Zhang M, Qi J, Sun X, Wang L, Li J (2019) Metal-organic framework-derived Hollow Co_3O_4 /Carbon as Efficient Catalyst for Peroxymonosulfate Activation. Chem Eng J 363:234–246. https://doi.org/10.1016/j.cej.2019.01.129
25. Nsh A, Aaja B, Ih C, Aaf A, Msa C, Rs D, Nhhh E (2021) Intensification of toxic chlorophenolic compounds degradation over efficient microwave-dried silica-doped tetragonal zirconia nanocatalysts. Chem Eng Process - Process Intensif 165:108469. https://doi.org/10.1016/j.cep.2021.108469
26. Peng L, Deng D, Guan M, Fang X, Zhu Q (2015) Remediation HCHs POPs-contaminated soil by activated persulfate technologies: Feasibility, impact of activation methods and mechanistic implications. Sep Purif Technol 150:215–222. https://doi.org/10.1016/j.seppur.2015.07.002
27. Pirsaheb M, Moradi S, Shahlaei M, Wang X, Farhadian N (2018) A new composite of nano zero-valent iron encapsulated in carbon dots for oxidative removal of bio-refractory antibiotics from water. J Clean Prod 209:1523–1532. https://doi.org/10.1016/j.jclepro.2018.11.175
28. Vipul G, Kant BN, Kumar RR (2021) Waste Water Air & Soil Pollution 232:326. https://doi.org/10.1007/s11270-021-05266-1. Remediation of Chlorophenolic Compounds from Paper Mill Effluent Using High-Quality Activated Carbon from Mixed Plastic
29. Vogel M, Georgi A, Kopinke FD, Mackenzie K (2019) Sulfidation of ZVI/AC composite leads to highly corrosion-resistant nanoremediation particles with extended life-time. Sci Total Environ 665:235–245. https://doi.org/10.1016/j.scitotenv.2019.02.136
30. Wang J, Wang S (2018) Activation of persulfate (PS) and peroxymonosulfate (PMS) and application for the degradation of emerging contaminants - ScienceDirect. Chem Eng J 334:1502–1517. https://doi.org/10.1016/j.cej.2017.11.059
31. Wang XH, Lin YC (2012) Phototransformation of Cephalosporin Antibiotics in an Aqueous Environment Results in Higher Toxicity. Environ Sci Technol 46:12417–12426. https://doi.org/10.1021/es301929e
32. Wang Y, Wang L, Zhang Y, Mao X, Xi B (2021) Perdisulfate-Assisted Advanced Oxidation of 2,4-Dichlorophenol by Bio-inspired Iron Encapsulated Biochar Catalyst. J Colloid Interface Sci 592:358–

370. https://doi.org/10.1016/j.jcis.2021.02.056
33. Wang YR, Tian DF, Chu W, Li MR, Lu XW (2019) Nanoscaled magnetic CuFe2O4 as an activator of peroxymonosulfate for the degradation of antibiotics norfloxacin. Sep Purif Technol 212:536–544. https://doi.org/10.1016/j.seppur.2018.11.051
34. Wu GC, Kong WJ, Gao Y, Kong Y, Dai ZG, Dan HB, Shang YN, Wang SQ, Yin FJ, yue QY, Gao BY (2021) Removal of chloramphenicol by sulfide-modified nanoscale zero-valent iron activated persulfate: Performance, salt resistance, and reaction mechanisms. Chemosphere 286:131876. https://doi.org/10.1016/j.chemosphere.2021.131876
35. Xl A, Ms A, Jl A, Ym A, Bga B, Hl B, Zhab C (2021) Resource utilization of piggery sludge to prepare recyclable magnetic biochar for highly efficient degradation of tetracycline through peroxymonosulfate activation. J Clean Prod 294. https://doi.org/10.1016/j. jclepro.2021.126372
36. Xu J, Cao Z, Wang Y, Zhang YL, Gao XY, Ahmed MB, Zhang J, Yang Y, Zhou JL, Lowry GV (2019) Distributing sulfidized nanoscale zerovalent iron onto phosphorus-functionalized biochar for enhanced removal of antibiotic florfenicol. Chem Eng J 359:713–722. https://doi.org/10.1016/j.cej.2018.11.180
37. Yousefi N, Pourfadakari S, Esmaeili S, Babaei AA (2019) Mineralization of high saline petrochemical wastewater using Sonoelectro-activated persulfate: Degradation mechanisms and reaction kinetics. Microchem J 147:1075–1082. https://doi.org/10.1016/j.microc.2019.04.020
38. Zhang P, Song D, Hao XJX, Sun Y, H (2021) Sulfidated zero valent iron as a persulfate activator for oxidizing organophosphorus pesticides (OPPs) in aqueous solution and aged contaminated soil columns. Chemosphere 281:130760. https://doi.org/10.1016/j.chemosphere.2021.130760
39. Zhao J, Zhang BT, Li J, Shi Y, Yang Z (2019a) Oxidative degradation of chloroxylenol in aqueous solution by thermally activated persulfate: Kinetics, mechanisms and toxicities. Chem Eng J 368:553–563. https://doi.org/10.1016/j.cej.2019.02.208
40. Zhao M, Zhou M, Li YC, Wang J, Gao B, Sato S, Feng K, Yin W, Igalavithana AD (2019b) Biochar-supported nZVI (nZVI/BC) for contaminant removal from soil and water: A critical review. J Hazard Mater 373:820–834. https://doi.org/10.1016/j.jhazmat.2019.03.080
41. Zhou Y, Zhang Y, Hu X (2020) Enhanced activation of peroxymonosulfate using oxygen vacancy-enriched FeCo2O4x spinel for 2,4-dichlorophenol removal: Singlet oxygen-dominated nonradical process. Colloids and Surfaces A Physicochemical and Engineering Aspects 597:124568. https://doi.org/ 10.1016/j.colsurfa.2020.124568
42. Zhu F, Wu Y, Liang Y, Li H, Liang (2020) Degradation mechanism of Norfloxacin in Water using Persulfate Activated by BC@nZVI/Ni. Chem Eng J 389:124276. https://doi.org/10.1016/j.cej.2020.124276

Figures

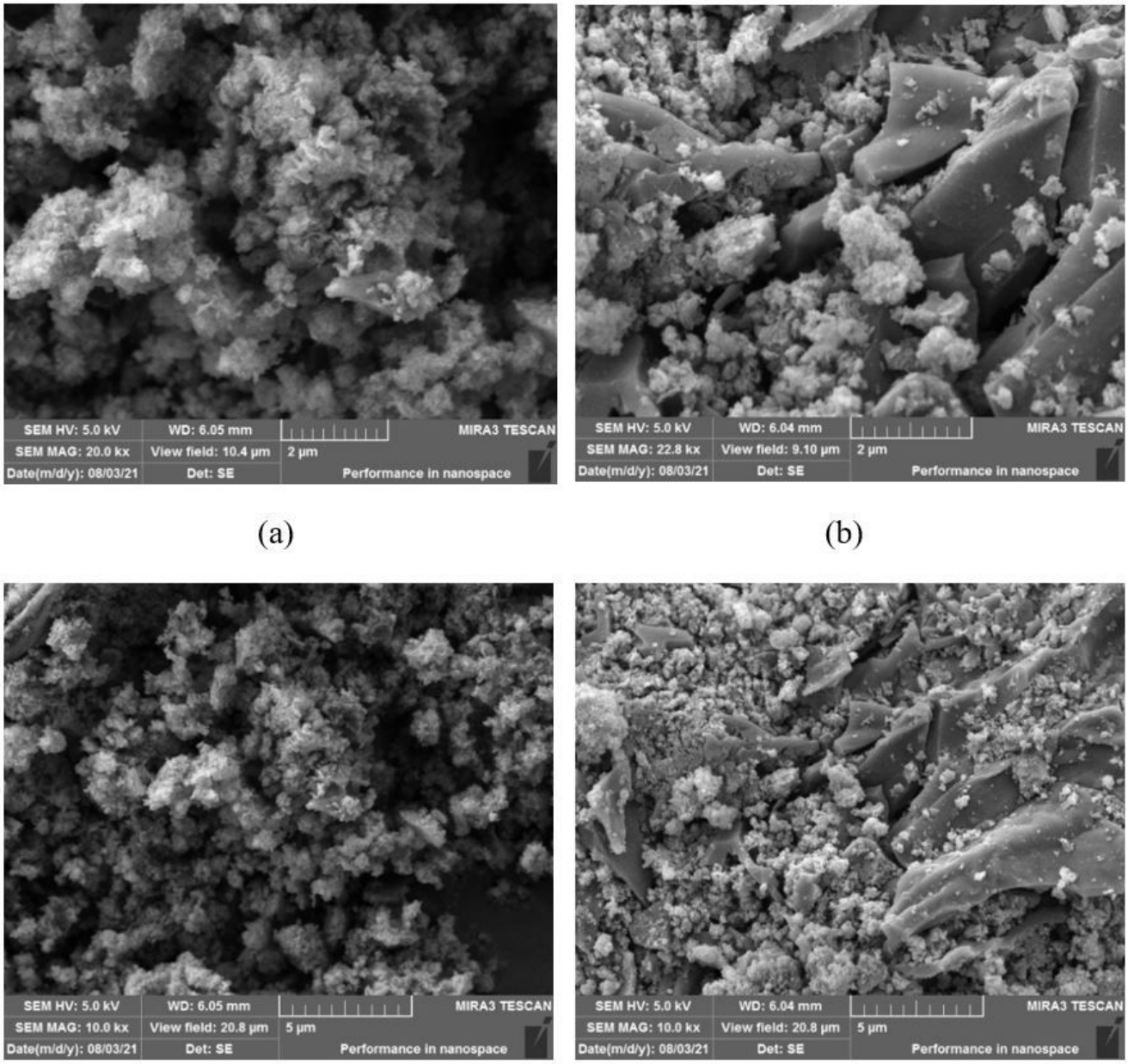

Figure 1

SEM images of BC@S-nZVI before and after reaction (a), (b) 2μm grade, (c), (d) 5μm grade

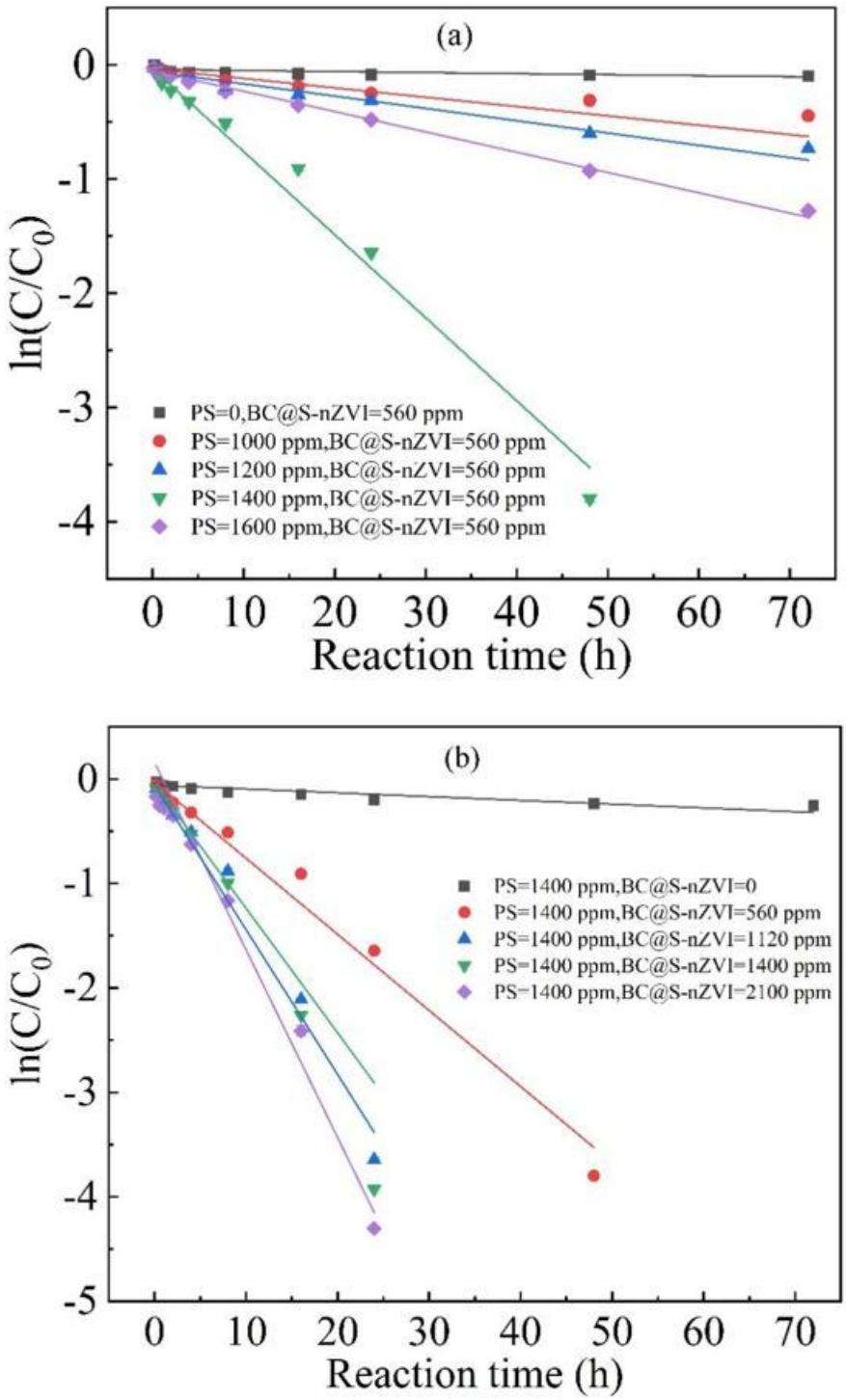

Figure 2

Effect of different activation systems on the degradation of 2-CP (a) different mass concentration of PS, (b) different mass concentration of BC@S-nZVI. Reaction condition: [2-CP]=20 ppm of 20 mL, T=30 °C, pH=5±0.2

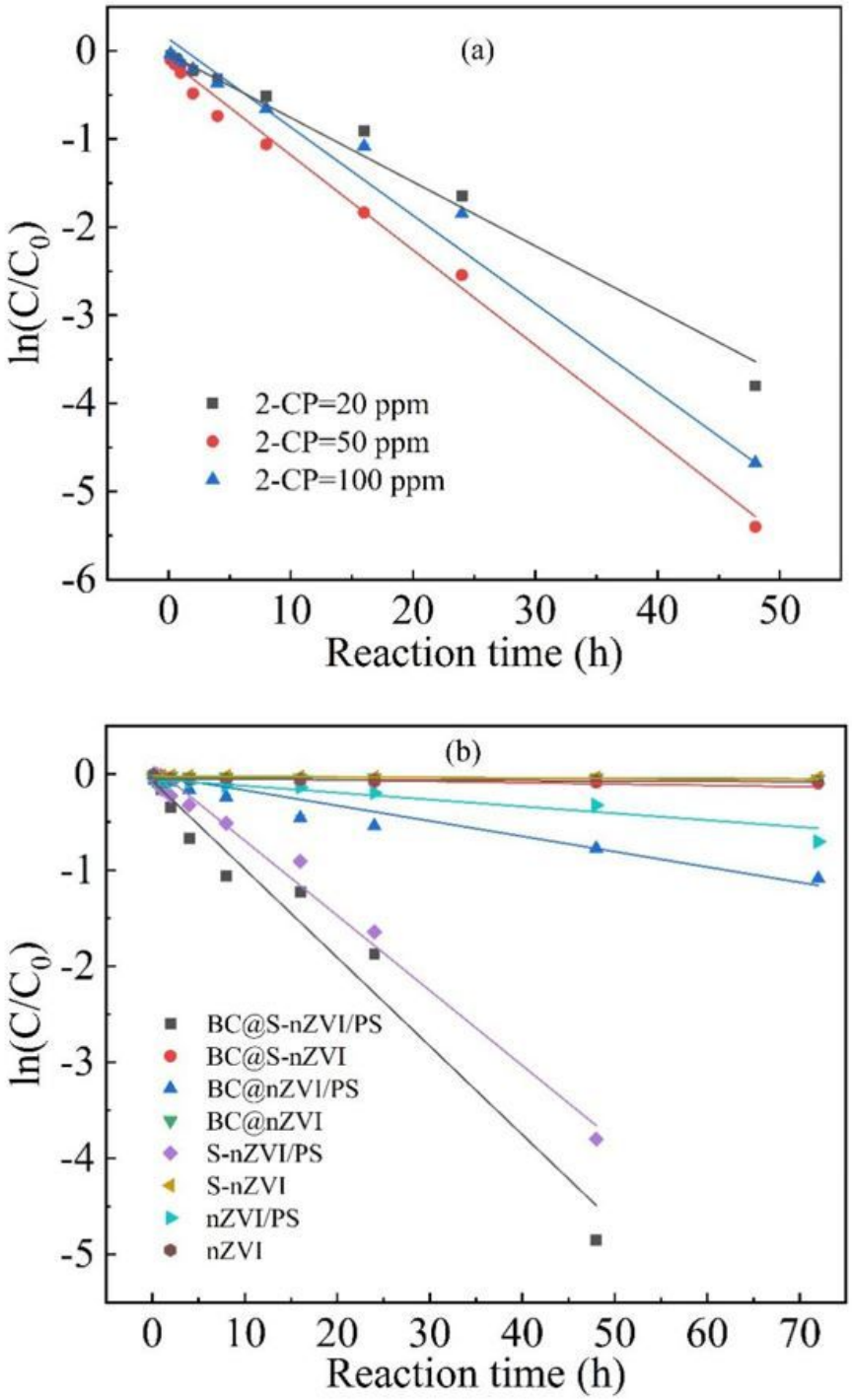

Figure 3

Verification of the optimum mass ratios (a) degradation effects of different initial concentration values of 2-CP, (b) degradation effects of various reaction systems. Reaction condition: mass ratio of PS to 2-CP equalled to 70, mass ratio of BC@S-nZVI to PS equalled to 0.4, T=30 °C, pH=5±0.2

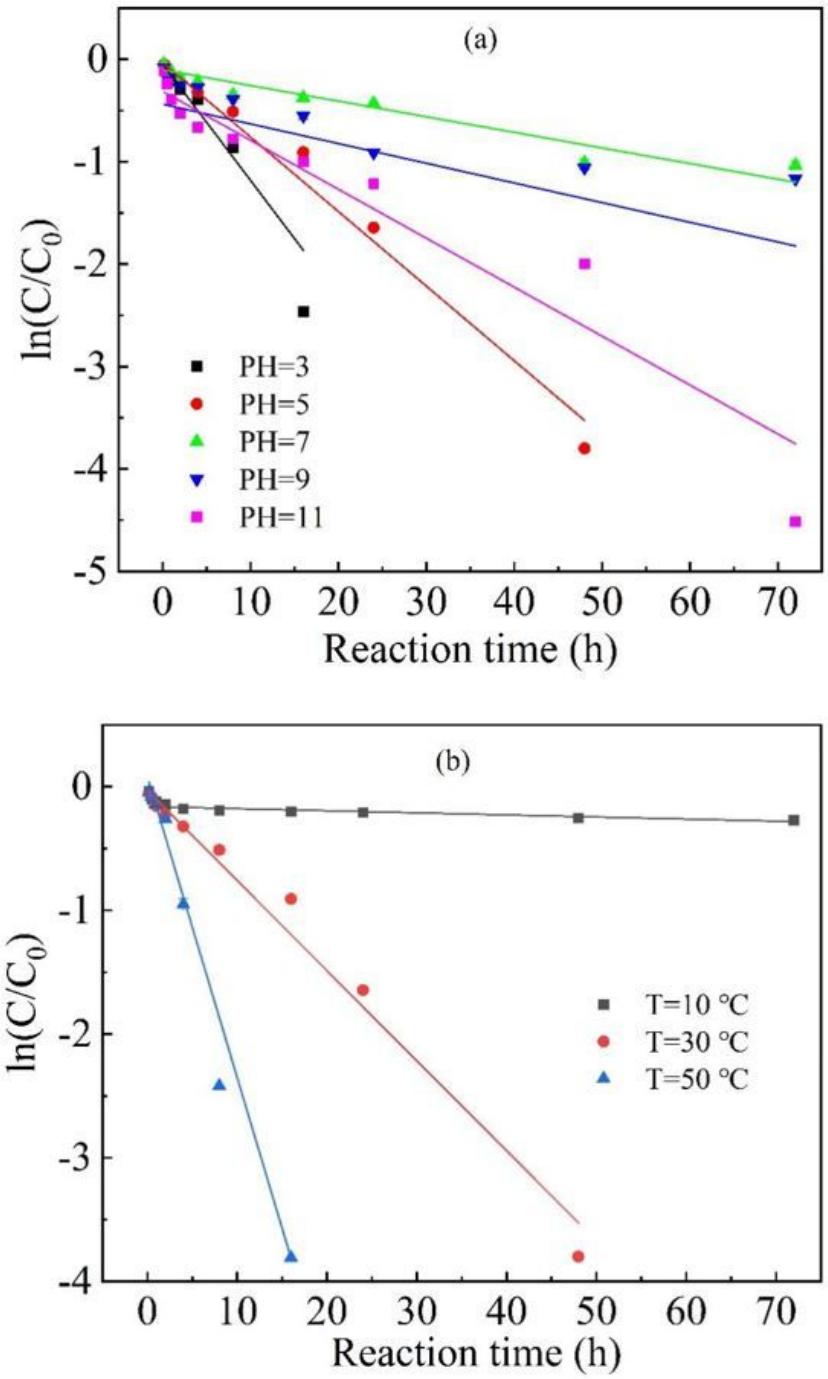

Figure 4

Effect of pH and temperature on the degradation of 2-CP (a) different values of pH. Reaction condition: [2-CP]=20 ppm of 20 mL, PS=1400 ppm, BC@S-nZVI=560 ppm, T=30 °C, (b) different values of temperature. Reaction condition: [2-CP]=20 ppm of 20 mL, PS=1400 ppm, BC@S-nZVI=560 ppm, pH=5±0.2

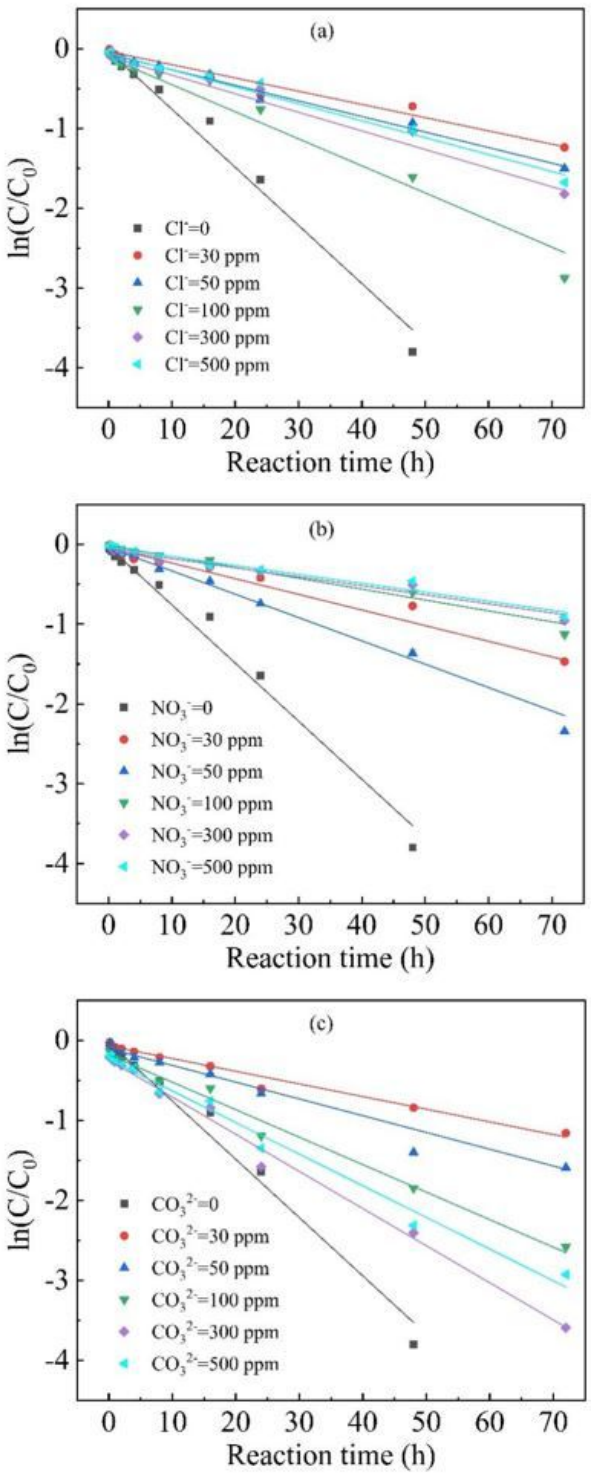

Figure 5

Effect of inorganic anions on the degradation of 2-CP (a) Cl^-, (b) NO_3^-, (c) CO_3^{2-}. Reaction condition: [2-CP]=20 ppm of 20 mL, PS=1400 ppm, BC@S-nZVI=560 ppm, T=30 °C, pH=5±0.2

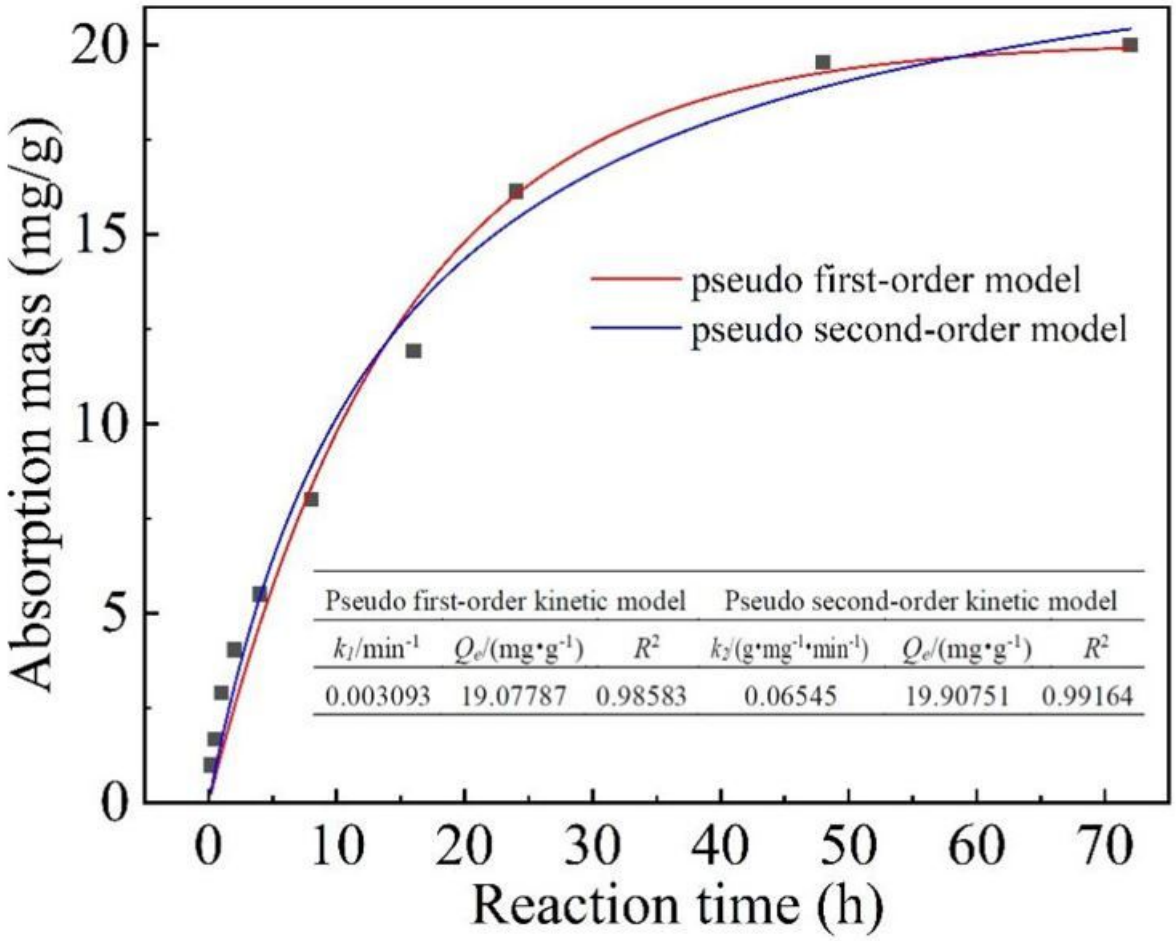

Figure 6

Adsorption kinetics simulation on the degradation of 2-CP. Reaction condition: [2-CP]=20 ppm of 20 mL, PS=1400 ppm, BC@S-nZVI=560 ppm, T=30 °C, pH=5±0.2

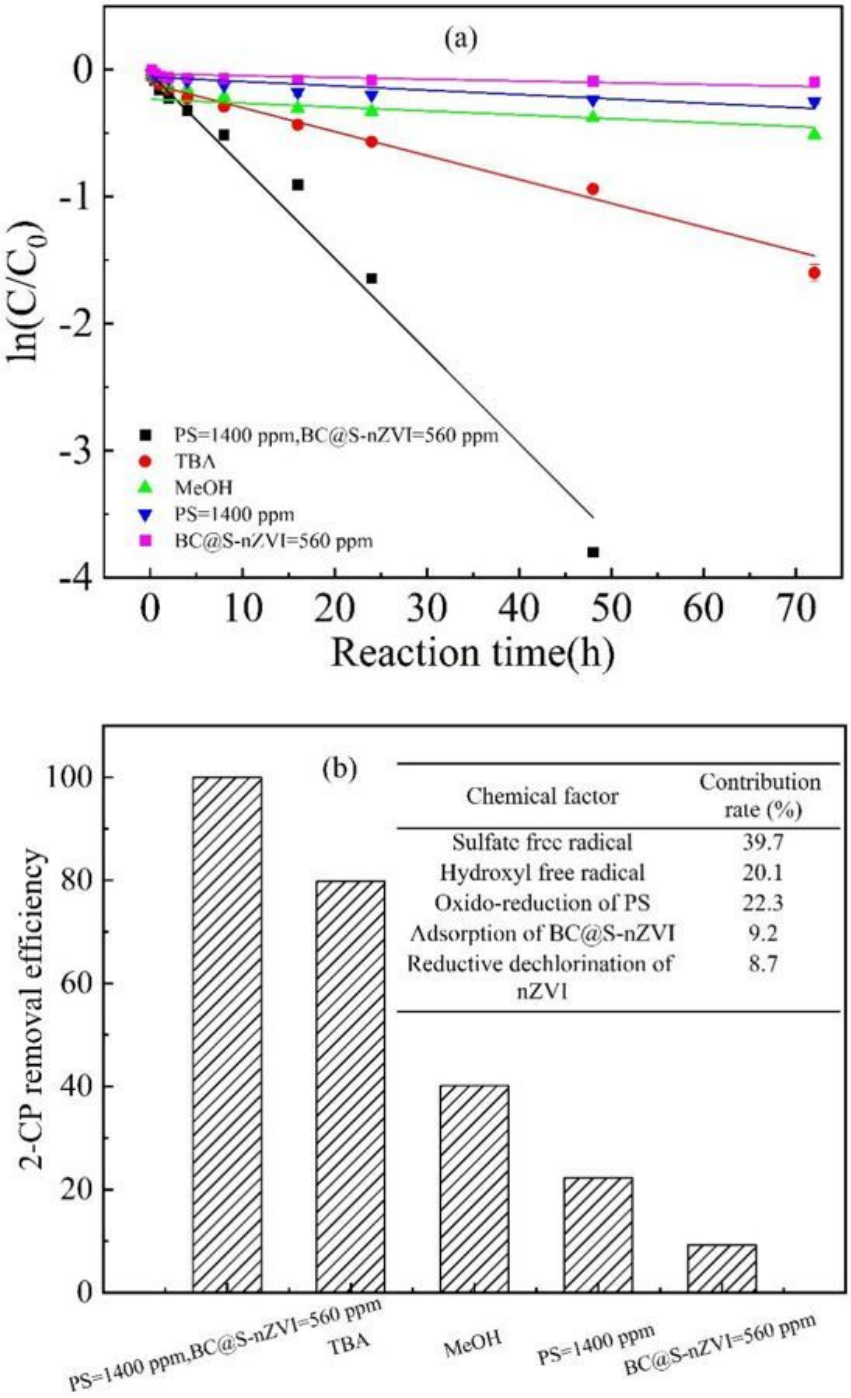

Figure 7

Contribution rate study of chemical factors (a) Degradation effect of different additives, (b) 2-CP removal efficiency of 72 h in each group. Reaction condition: [2-CP]=20 ppm of 20 mL, T=30 ℃, pH=5±0.2